Biochemical and Biophysical Research Communications 423 (2012) 55–59

Contents lists available at SciVerse ScienceDirect

Biochemical and Biophysical Research Communications

journal homepage: www.elsevier.com/locate/ybbrc

Changes of calcium channel mRNA, protein and current in NG108-15 cells after cell differentiation

Jinxu Liu [a], Huiyin Tu [a], Dongze Zhang [a], Yu-Long Li [a,b,*]

[a] Department of Emergency Medicine, University of Nebraska Medical Center, Omaha, NE 68198-5850, USA
[b] Department of Cellular & Integrative Physiology, University of Nebraska Medical Center, Omaha, NE 68198, USA

ARTICLE INFO

Article history:
Received 10 May 2012
Available online 22 May 2012

Keywords:
Acetylcholine
Ca^{2+} channel
NG108-15 cell
Patch clamp
Real-time RT-PCR
Western blot

ABSTRACT

Based on the characteristics of differentiated NG108-15 cells (cell membrane excitability, acetylcholine release, and activities of choline acetyltransferase and acetylcholinesterase), NG108-15 cells are extensively used to explore neuronal functions as a cholinergic cell line. In the present study, differentiation-induced alterations of voltage-gated Ca^{2+} channel mRNA, protein, and current were investigated in the NG108-15 cells. Real-time PCR, Western blot, and whole-cell patch-clamp data showed that differentiation caused mRNA, protein, and ion current changes of all Ca^{2+} channel subunits. However, the changes of mRNA, protein, and ion current are inconsistent in all Ca^{2+} channel subunits. Especially, P/Q- and R-type Ca^{2+} channel proteins do not form the functional P/Q- and R-type Ca^{2+} channels even if the mRNA and protein of P/Q- and R-type Ca^{2+} channels can be detected in NG108-15 cells. These results indicate that differentiation can modulate gene transcription, protein translation, and post-translation of the Ca^{2+} channels to induce the alteration of the Ca^{2+} ion currents in NG108-15 cells. From these data, we understand that combining real-time PCR, Western blot, and patch-clamp techniques can comprehensively unveil the modulation of the Ca^{2+} channels.

1. Introduction

Cholinergic neurons releasing the neurotransmitter acetylcholine are found extensively in parasympathetic nervous system, preganglionic neurons of the sympathetic nervous system, basal forebrain, brain stem complexes, and neuromuscular junctions. Exploring cellular and molecular characteristics of the cholinergic neurons is very important to understand acetylcholine release and neural control of the whole body function in vertebrates. However, the structural complexity and minute sample of these tissues limit some key cellular and molecular measurements. NG108-15 cell line was formed by fusing mouse N18TG2 neuroblastoma cells with rat C6-BU-1 glioma cells in the presence of inactivated Sendai virus [9]. After differentiation, this cell line develops the ultimate neural property of acetylcholine release depending on cell depolarization, and presents neurite extension, membrane excitability, and specific activities of choline acetyltransferase and acetylcholinesterase [4,5,14]. Therefore, differentiated NG108-15 cells are thought to be a cholinergic cell line for studying neural functions.

Calcium ions play a key role in the control of cellular function in all tissues. Normally intracellular free calcium concentration is very low compared with extracellular calcium concentration. Increasing intracellular free calcium concentration can initiate muscle contraction and neurotransmitter release. Calcium influx is mainly controlled by voltage-gated Ca^{2+} channels, especially in excitable cells. Therefore, voltage-gated Ca^{2+} channels are involved in the neuronal excitability and neurotransmission in the central and peripheral nervous system [12,19]. Although electrophysiological alterations of the voltage-gated Ca^{2+} channels were investigated in differentiated NG108-15 cells [6,7], mRNA and protein expression of each voltage-gated calcium channel subunit are not reported in NG108-15 cells. Here we investigated the time-course for differentiation-induced changes of Ca^{2+} channel mRNA, protein, and current in NG108-15 cells.

2. Methods

2.1. Cell culture and differentiation

The neuroblastoma × glioma NG108-15 cell line was obtained from the American Type Culture Collection (ATCC, Manassas, VA). NG108-15 cells were cultured in plastic flasks containing 90% Dulbecco's modified Eagle's medium (DMEM) and 10% fetal bovine serum (FBS) supplemented with 100 μM hypoxanthine, 0.4 μM aminopterin, 16 μM thymidine (HAT) and antibiotics in a humidified

Abbreviations: 4-AP, 4-aminopyridine; dBcAMP, N^6,2′-*O*-dibutyryladenosine 3′,5′-cyclic monophosphate; Ca_v, voltage-gated calcium; DMEM, Dulbecco's modified Eagle's medium; FBS, fetal bovine serum; SDS, sodium dodecyl sulfate; TEA, tetraethylammonium; TTX, tetrodotoxin.

* Corresponding author at: Department of Emergency Medicine, University of Nebraska Medical Center, Omaha, NE 68198-5850, USA. Fax: +1 402 559 9659.
E-mail address: yulongli@unmc.edu (Y.-L. Li).

0006-291X/$ - see front matter © 2012 Elsevier Inc. All rights reserved.
http://dx.doi.org/10.1016/j.bbrc.2012.05.076

atmosphere of 95% air-5% CO_2 at 37 °C. Cells were subcultured by gentle trypsinization and plated at a density of 1×10^4 cells/cm^2 on either a 60 mm plastic dish or a 35 mm plastic dish containing glass cover slips. Differentiation was induced by culturing the cells in a serum-free medium composed of DMEM, N2 supplements, 1 mM dBcAMP (Sigma–Aldrich, St. Louis, MO) and antibiotics. Cells were used for experiments after 0–9 days of differentiation.

2.2. Real-time RT-PCR

Total RNA of NG108-15 cells was extracted using the Trizol reagent (Invitrogen, Carlsbad, CA) according the manufacturer's instructions. First-strand cDNA was synthesized using the iScript cDNA synthesis kit (Bio-Rad, Hercules, CA). Changes in the mRNA expression of Ca_v subunits were examined by real-time RT-PCR with an ABI StepOnePlus Real-Time PCR System (Applied Biosystems, Foster City, CA). cDNA was amplified using iQ SYBR green supermix (Bio-Rad) in the presence of specific primers for $Ca_v1.2$, $Ca_v1.3$, $Ca_v2.1$, $Ca_v2.2$, $Ca_v2.3$, $Ca_v3.1$, $Ca_v3.2$, $Ca_v3.3$ and RPL19 (Table 1). The PCR conditions were as follows: 95 °C for 10 min, followed by 40 cycles consisting of 95 °C for 15 s and 60 °C for 1 min. The quantification was performed by the comparative CT (cycle threshold) method [13], using housekeeping gene RPL19 as internal control.

2.3. Western blot

The protein of NG108-15 cell lysates was extracted with the lysing buffer (10 mM Tris, 1 mM EDTA, 1% SDS, pH 7.4) plus protease inhibitor cocktail (Sigma–Aldrich, 100 μl/ml). Total protein concentration was determined using a bicinchoninic acid protein assay kit (Thermo Fisher Scientific, Rockford, IL). Equal amounts of the protein samples were loaded and then separated on a 10% sodium dodecyl sulfate (SDS)–polyacrylamide gel. The proteins of these samples were electrophoretically transferred to PVDF membrane. The membrane was probed with rabbit antibodies against Ca^{2+} channel subunits ($Ca_v1.2$, $Ca_v1.3$, $Ca_v2.1$, $Ca_v2.2$, $Ca_v2.3$, $Ca_v3.1$, $Ca_v3.2$, $Ca_v3.3$; Alomone Labs, Jerusalem, Israel) and a peroxidase-conjugated goat anti-rabbit IgG (Thermo Fisher Scientific, Rockford, IL). The signal was detected using enhanced chemiluminescence substrate (Thermo Fisher Scientific, Rockford, IL) and the bands were analyzed using UVP bioimaging system. The membrane was reprobed with mouse anti-GAPDH antibody (Santa Cruz Biotechnology, Santa Cruz, CA) and normalizing target protein intensity to that of GAPDH.

Table 1
Primer sequences for real-time RT-PCR.

Gene accession	Primer name	Primer sequence (5′–3′)
NM_009781	$Ca_v1.2$-forward	TGCTGTGTCTGACCCTGAAG
	$Ca_v1.2$-reverse	CGTCTTCCGGAAAGGGAATA
NM_028981	$Ca_v1.3$-forward	AACTTTCCGCTCGGTGGCTGT
	$Ca_v1.3$-reverse	TCGGGCATCAGTCTCTTGGGAG
NM_007578	$Ca_v2.1$-forward	CGACCGGGATCGCTACGCAC
	$Ca_v2.1$-reverse	GGCTGGGCTTCCACTGACGG
NM_007579	$Ca_v2.2$-forward	TCCTCATGTTTGCCATCATC
	$Ca_v2.2$-reverse	ACAGGGAAAGTCACCCACAG
NM_009782	$Ca_v2.3$-forward	GACCCTAGCTCTATGCGACG
	$Ca_v2.3$-reverse	GCCGCGACTTGTAAGTGTTT
NM_009783	$Ca_v3.1$-forward	CCTGAGAATTTCAGCCTCCC
	$Ca_v3.1$-reverse	GATCGCATGCCGTTCTCC
NM_021415	$Ca_v3.2$-forward	ATGTACTCACTGGCTGTGACC
	$Ca_v3.2$- reverse	GAGTCCAAAAGAGTGTGGGC
NM_001044308	$Ca_v3.3$-forward	TCCCGGAATCTGAGGCGTGGG
	$Ca_v3.3$-reverse	AGCCCTTGGCATGGACGTGG
NM_009078	RPL19-forward	CTGAAGGTCAAAGGGAATGTGTTC
	RPL19-reverse	TTCGTGCTTCCTTGGTCTTAGAC

2.4. Recording of voltage-gated Ca^{2+} channel currents

Ca^{2+} currents were recorded by the whole-cell patch-clamp technique using Axonpatch 200B patch-clamp amplifier (Axon Instruments, Sunnyvale, CA). Resistance of the patch pipette was 2–4 MΩ when filled with (in mM) 120 CsCl, 1 $CaCl_2$, 40 HEPES, 11 EGTA, 4 MgATP, 0.3 Tris-GTP, 14 creatine phosphate, and 0.1 leupeptin, pH 7.3 with CsOH. The extracellular solution consisted of (in mM): 140 tetraethylammonium (TEA)-Cl, 5 $BaCl_2$, 1 $MgCl_2$, 10 HEPES, 0.001 TTX, 2 4-aminopyridine (4-AP), and 10 glucose, pH 7.4 with TEA-OH. Series resistance of 3–10 MΩ was electronically compensated 60–85%. Junction potential was calculated to be + 7.9 mV using pClamp 10.2 software, and all values of membrane potential given throughout were corrected using this value. Current traces were sampled at 10 kHz and filtered at 5 kHz. To separate the high voltage-activated (L, P/Q, N and R-type) and low voltage-activated (T-type) Ca^{2+} currents, different holding potentials were used. Whole Ca^{2+} currents were first evoked from a holding potential of −80 mV by stepping to voltages between −60 and + 60 mV in 5 mV steps for 200 ms. High voltage-activated Ca^{2+} currents were then recorded from a holding potential of −40 mV by stepping to voltages between −40 and + 60 mV in 5 mV steps for 200 ms. Subtraction of the high voltage-activated Ca^{2+} currents from the whole Ca^{2+} currents yielded the low voltage-activated Ca^{2+} currents. L- and N-type Ca^{2+} currents were further separated from high voltage-activated Ca^{2+} currents by exposed the cells to 10 μM nifedipine (a specific L-type Ca^{2+} channel blocker) or 1 μM ω-conotoxin GVIA (a specific N-type Ca^{2+} channel blocker) in bath solution. Peak currents were measured

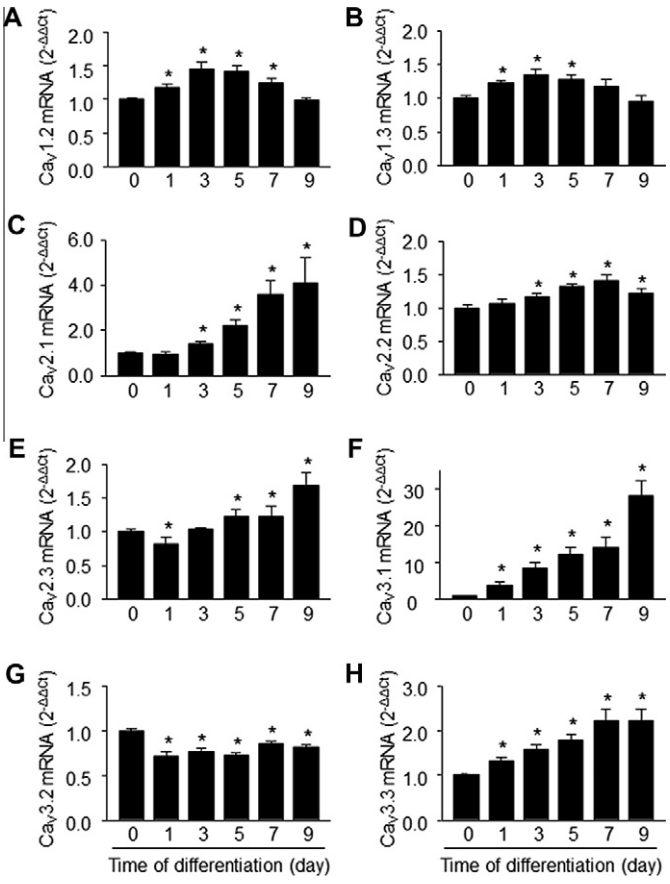

Fig. 1. Expression of mRNA for Ca^{2+} channel subunits before and after differentiation in NG108-15 cells, measured by real-time RT-PCR. Data are means ± SEM, $n = 4$ time measurements in each time-point. $^*P < 0.05$ vs. 0 day of differentiation (non-differentiated condition).

for each test potential and current density was calculated by dividing peak current by cell membrane capacitance. pClamp 10.2 programs (Axon Instruments) were used for data acquisition and analysis. All experiments were done at room temperature.

2.5. Data analysis

All data are presented as means ± SEM. SigmaStat 3.5 was used for data analysis. A one-way ANOVA, with a Bonferroni procedure for post hoc was used in comparisons of mRNA, protein, and ion current of Ca^{2+} channel subunits. All data were confirmed by the Kolmogorov–Smirnov test to fit reasonably within normal distribution and equal variance was confirmed by the Levene test. Statistical significance was accepted when $P < 0.05$.

3. Results and discussion

3.1. Expression of Ca^{2+} channel mRNA in NG108-15 cells

Until now, five subtypes (L, P/Q, N, R and T) of the voltage-gated Ca^{2+} channels have been functionally characterized in neurons [16,17]. A pore-forming α1 subunit contained in all Ca^{2+} channels determines the biophysical and pharmacological properties of the Ca^{2+} channels including generation of the Ca^{2+} currents in the absence of the other subunits [1,15]. There are three major families of α1 subunits: (1) Ca_v1 ($Ca_v1.1$, $Ca_v1.2$, and $Ca_v1.3$) family encodes L-type of the Ca^{2+} channels; (2) Ca_v2 family encodes P/Q ($Ca_v2.1$), N ($Ca_v2.2$), and R ($Ca_v2.3$) types of the Ca^{2+} channels; (3) Ca_v3 ($Ca_v3.1$, $Ca_v3.2$, and $Ca_v3.3$) family encodes T type of the Ca^{2+} channels [1,2]. In neurons, gene expression of L-type Ca^{2+} channels is controlled by $Ca_v1.2$, and $Ca_v1.3$ but not $Ca_v1.1$ [8,11]. Using real-time RT-PCR analysis, therefore, we measured the mRNA expression of Ca^{2+} channel α1 subunits those should be existed in NG108-15 cells, which are shown in Fig. 1.

The mRNA expression of Ca_v1 family ($Ca_v1.2$, and $Ca_v1.3$) increased in differentiated NG108-15 cells, which peaked at third day of differentiation (Fig. 1A and B). The mRNA level of Ca_v2 family ($Ca_v2.1$, $Ca_v2.2$, and $Ca_v2.3$) significantly increased with differentiating time-dependent manner (Fig. 1C–E). For Ca_v3 family ($Ca_v3.1$, $Ca_v3.2$, and $Ca_v3.3$), the mRNA expression of $Ca_v3.1$and $Ca_v3.3$ enhanced with differentiating time-dependent manner, whereas $Ca_v3.2$ mRNA level was decreased by differentiation (Fig. 1F–H). These results indicate that differentiation induced different changes of Ca^{2+} channel α1 subunits in NG108-15 cells via modulating gene transcription.

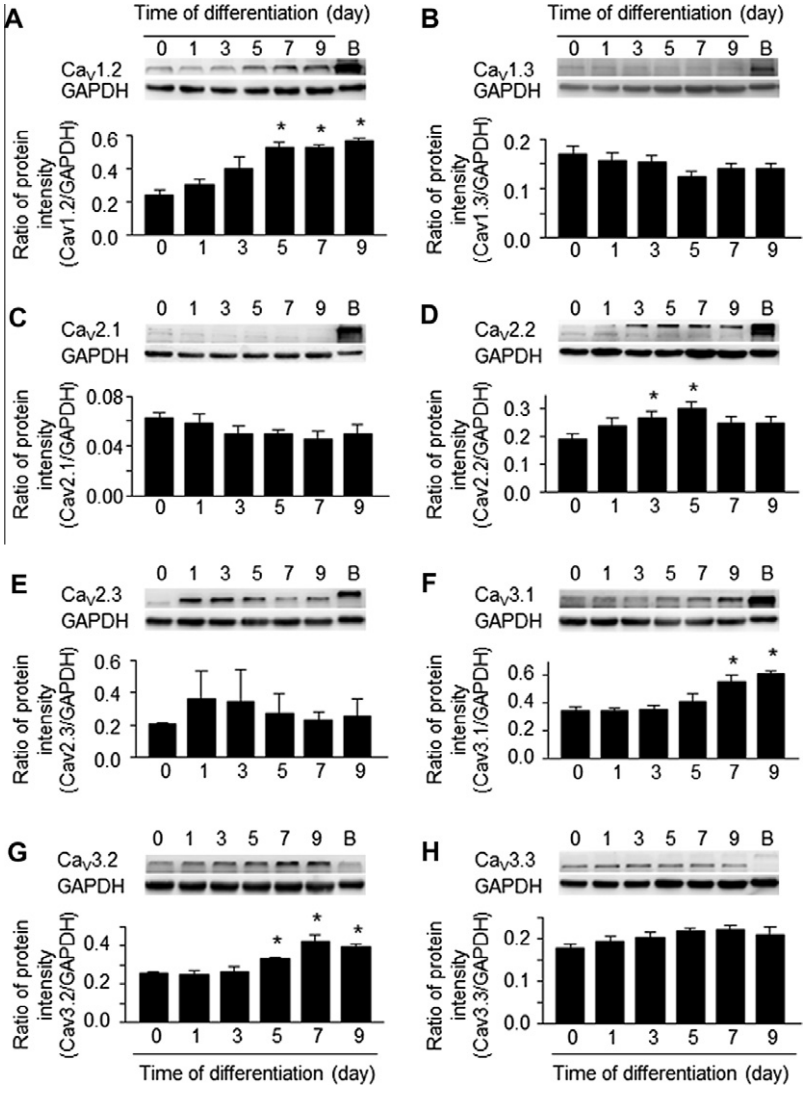

Fig. 2. Expression of protein for Ca^{2+} channel subunits before and after differentiation in NG108-15 cells, measured by Western blot analysis. A positive Ca^{2+} channel protein control (B, mouse brainstem) is shown on the same gel. Data are means ± SEM, $n = 4$ time measurements in each time-point. $^*P < 0.05$ vs. 0 day of differentiation (non-differentiated condition).

3.2. Expression of Ca^{2+} channel protein in NG108-15 cells

We also used western blot analysis to measure the protein expression of Ca^{2+} channel α1 subunits in NG108-15 cells. Additionally the protein expression of Ca^{2+} channel α1 subunits in mouse brainstem was also measured on the same gel as a positive Ca^{2+} channel protein control. As shown in Fig. 2, the level of $Ca_v1.2$ protein increased with differentiating time-dependent manner whereas the level of $Ca_v1.3$ protein was insignificantly affected by differentiation in Ca_v1 family (Fig. 2A–B). In Ca_v2 family, the level of $Ca_v2.2$ protein significantly enhanced at third and fifth days, but differentiation did not influence the protein level of $Ca_v2.1$ and $Ca_v2.3$ (Fig. 2C–E). In Ca_v3 family, NG108-15 cell differentiation increased the protein level of $Ca_v3.1$ and $Ca_v3.2$ with time-dependent manner but did not affect the protein level of $Ca_v3.3$ (Fig. 2F–H). From these data, we found that differentiation-induced changes of the proteins (Fig. 2) are not consistent with differentiation-caused alterations of the mRNAs (Fig. 1) in Ca^{2+} channel α1 subunits in NG108-15 cells. Real-time RT-PCR and Western blot results (Figs. 1 and 2) suggest that differentiation regulates not only gene transcription but also protein translation of Ca^{2+} channel α1 subunits in NG108-15 cells.

3.3. Voltage-gated Ca^{2+} channel currents in NG108-15 cells

Based on biophysical differences, Ca^{2+} channels are classified into high voltage-activated Ca^{2+} channels (including L, P/Q, N, and R subtypes) and low voltage-activated Ca^{2+} channels (only T subtype) [1–3,11]. In patch-clamp whole-cell recording, T-type Ca^{2+} currents ($Ca_v3.1$, $Ca_v3.2$, and $Ca_v3.3$) were obtained by subtracting high voltage-activated Ca^{2+} currents (recording in a holding potential of −40 mV) from whole Ca^{2+} currents (recording in a holding potential of −80 mV) (Fig. 3). There is a small T-type Ca^{2+} current in non-differentiated NG-108-15 cells. After 5 days of differentiation, T-type Ca^{2+} currents did not changed compared to non-differentiated condition. However, a significant increase of T-type Ca^{2+} currents was caused after 9 days of differentiation (Fig. 3A–B).

High voltage-activated Ca^{2+} currents (including L, P/Q, N, and R subtypes) were recorded in a holding potential of −40 mV. After

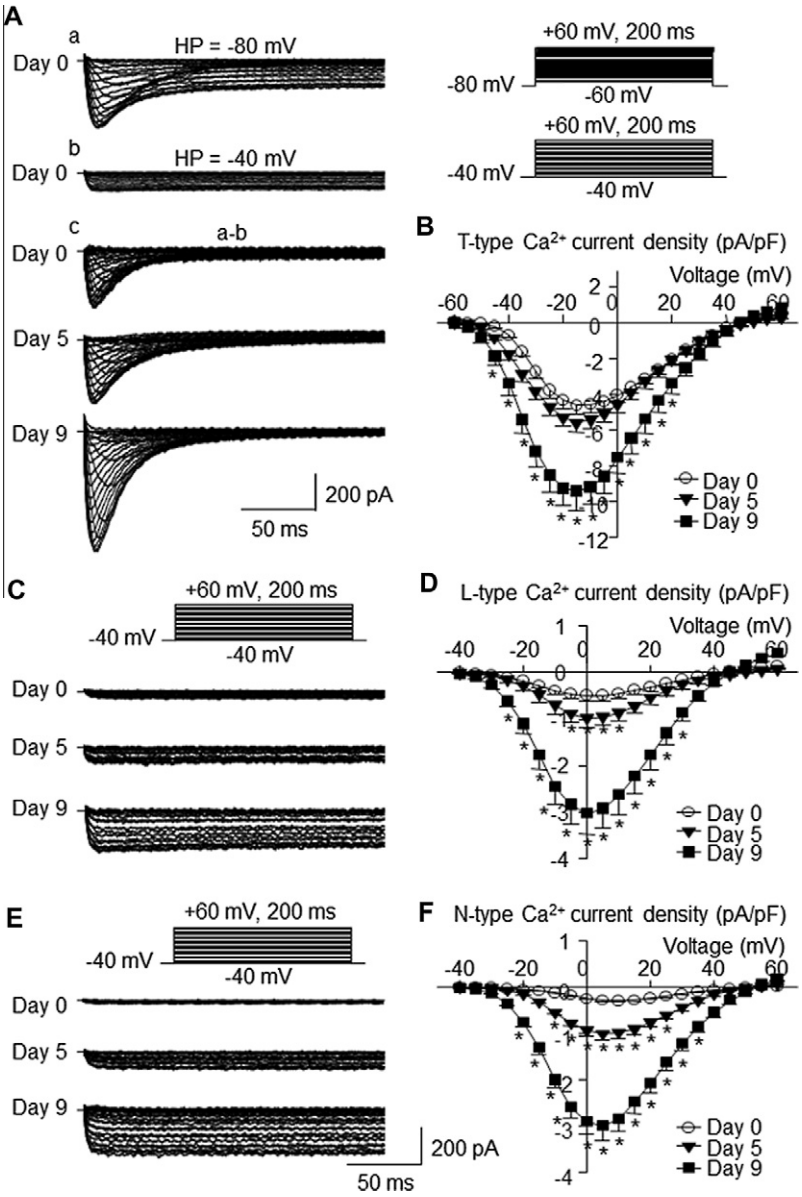

Fig. 3. Original recordings (A, C, and E) and current–voltage (I–V) curves (B, D, and F) of the voltage-gated Ca^{2+} currents before and after differentiation in NG108-15 cells, measured by whole-cell patch-clamp technique. Data are means ± SEM, $n = 10$ cells in each time-point. $^*P < 0.05$ vs. 0 day of differentiation (non-differentiated condition).

co-treatment with saturating concentration of nifedipine (10 μM, specific L-type Ca^{2+} channel blocker) and ω-conotoxin GVIA (1 μM, specific N-type Ca^{2+} channel blocker) [10,12,18], high voltage-activated Ca^{2+} currents were totally inhibited (data not shown). These results suggest that the protein of $Ca_v2.1$ and $Ca_v2.3$ doesnot assemble the functional P/Q- and R-type Ca^{2+} channels to produce the high voltage-activated Ca^{2+} currents although the mRNA and protein of $Ca_v2.1$ and $Ca_v2.3$ could be detected (Figs. 1 and 2). Additionally we also consider that L-type ($Ca_v1.2$ and $Ca_v1.3$) and N-type ($Ca_v2.2$) Ca^{2+} channels are involved in the production of the high voltage-activated Ca^{2+} currents in NG108-15 currents.

After 5 days of differentiation, L-type and N-type Ca^{2+} currents were mildly increased ($p < 0.05$ vs. non-differentiation, Fig. 3). After 9 days of differentiation, L-type and N-type Ca^{2+} currents were further increased (Fig. 3). However, differentiation-induced protein expression of N-type ($Ca_v2.2$) Ca^{2+} channels peaked at the fifth day of differentiation. Based on these results, therefore, we can assume that differentiation also triggers post-translational modulation of Ca^{2+} channels in NG108-15 cells.

In conclusion, differentiation can induce the alterations of Ca^{2+} channel mRNA, protein and current in NG108-15 cells although these changes are inconsistent. These data suggest that differentiation can affect transcription, translation, and post-translational modulation of the Ca^{2+} channels to change the Ca^{2+} ion currents. Therefore, we should combine real-time PCR, western blot, and patch-clamp data to analyze the modulation of the Ca^{2+} channels.

References

[1] E.E. Benarroch, Neuronal voltage-gated calcium channels: brief overview of their function and clinical implications in neurology, Neurology 74 (2010) 1310–1315.

[2] W.A. Catterall, Structure and regulation of voltage-gated Ca^{2+} channels, Annu. Rev. Cell Dev. Biol. 16 (2000) 521–555.

[3] S. Dai, D.D. Hall, J.W. Hell, Supramolecular assemblies and localized regulation of voltage-gated ion channels, Physiol. Rev. 89 (2009) 411–452.

[4] M.P. Daniels, B. Hamprecht, The ultrastructure of neuroblastoma glioma somatic cell hybrids. Expression of neuronal characteristics stimulated by dibutyryl adenosine 3′,5′ cyclic monophosphate, J. Cell Biol. 63 (1974) 691–699.

[5] V. Dolezal, X. Castell, M. Tomasi, M.F. Diebler, Stimuli that induce a cholinergic neuronal phenotype of NG108-15 cells upregulate ChAT and VAChT mRNAs but fail to increase VAChT protein, Brain Res. Bull. 54 (2001) 363–373.

[6] R. Eckert, J. Hescheler, D. Krautwurst, G. Schultz, W. Trautwein, Calcium currents of neuroblastoma x glioma hybrid cells after cultivation with dibutyryl cyclic AMP and nickel, Pflugers Arch. 417 (1990) 329–335.

[7] S.B. Freedman, G. Dawson, M.L. Villereal, R.J. Miller, Identification and characterization of voltage-sensitive calcium channels in neuronal clonal cell lines, J. Neurosci. 4 (1984) 1453–1467.

[8] A. Ghosh, M.E. Greenberg, Calcium signaling in neurons: molecular mechanisms and cellular consequences, Science 268 (1995) 239–247.

[9] B. Hamprecht, Structural, electrophysiological, biochemical, and pharmacological properties of neuroblastoma–glioma cell hybrids in cell culture, Int. Rev. Cytol. 49 (1977) 99–170.

[10] S.W. Jeong, R.D. Wurster, Calcium channel currents in acutely dissociated intracardiac neurons from adult rats, J. Neurophysiol. 77 (1997) 1769–1778.

[11] D. Lipscombe, J.Q. Pan, A.C. Gray, Functional diversity in neuronal voltage-gated calcium channels by alternative splicing of Ca(v)alpha1, Mol. Neurobiol. 26 (2002) 21–44.

[12] J. Liu, H. Tu, H. Zheng, L. Zhang, T.P. Tran, R.L. Muelleman, Y.L. Li, Alterations of calcium channels and cell excitability in intracardiac ganglion neurons from type 2 diabetic rats, Am. J. Physiol Cell Physiol. 302 (2012) C1119–C1127.

[13] K.J. Livak, T.D. Schmittgen, Analysis of relative gene expression data using real-time quantitative PCR and the 2(-Delta Delta C(T)) Method, Methods 25 (2001) 402–408.

[14] R. McGee, P. Simpson, C. Christian, M. Mata, P. Nelson, M. Nirenberg, Regulation of acetylcholine release from neuroblastoma x glioma hybrid cells, Proc. Natl. Acad. Sci. USA 75 (1978) 1314–1318.

[15] E. Perez-Reyes, H.S. Kim, A.E. Lacerda, W. Horne, X.Y. Wei, D. Rampe, K.P. Campbell, A.M. Brown, L. Birnbaumer, Induction of calcium currents by the expression of the alpha 1-subunit of the dihydropyridine receptor from skeletal muscle, Nature 340 (1989) 233–236.

[16] R.W. Tsien, D. Lipscombe, D. Madison, K. Bley, A. Fox, Reflections on Ca(2+)-channel diversity, 1988–1994, Trends Neurosci. 18 (1995) 52–54.

[17] R.W. Tsien, D. Lipscombe, D.V. Madison, K.R. Bley, A.P. Fox, Multiple types of neuronal calcium channels and their selective modulation, Trends Neurosci. 11 (1988) 431–438.

[18] R. Wang, Y. Wu, G. Tang, L. Wu, S.T. Hanna, Altered L-type Ca(2+) channel currents in vascular smooth muscle cells from experimental diabetic rats, Am. J. Physiol Heart Circ. Physiol. 278 (2000) H714–H722.

[19] Z.J. Xu, D.J. Adams, Voltage-dependent sodium and calcium currents in cultured parasympathetic neurones from rat intracardiac ganglia, J. Physiol. 456 (1992) 425–441.